Design, Synthesis, and Cocrystal Structure of a Nonpeptide Src SH2 Domain Ligand

Mark S. Plummer,* Debra R. Holland, Aurash Shahripour, Elizabeth A. Lunney, James H. Fergus, James S. Marks, Patrick McConnell, W. Thomas Mueller, and Tomi K. Sawyer

Departments of Chemistry, Biochemistry, and Biotechnology, Parke-Davis Pharmaceutical Research Division, Warner-Lambert Company, 2800 Plymouth Road, Ann Arbor, Michigan 48105

Received June 17, 1997[⊗]

The specific association of an SH2 domain with a phosphotyrosine (pTyr)-containing sequence of another protein precipitates a cascade of intracellular molecular interactions (signals) which effect a wide range of intracellular processes. The nonreceptor tyrosine kinase Src, which has been associated with breast cancer and osteoporosis, contains an SH2 domain. Inhibition of Src SH2−phosphoprotein interactions by small molecules will aid biological proof-of-concept studies which may lead to the development of novel therapeutic agents. Structure-based design efforts have focused on reducing the size and charge of Src SH2 ligands while increasing their ability to penetrate cells and reach the intracellular Src SH2 domain target. In this report we describe the synthesis, binding affinity, and Src SH2 cocrystal structure of a small, novel, nonpeptide, urea-containing SH2 domain ligand.

Introduction

The pp60^{c-src} (Src) protein is a nonreceptor tyrosine kinase which is characterized by an N-terminal unique domain followed by two Src homology domains, SH3 and SH2, a catalytic kinase (or SH1) domain, and a short C-terminal regulatory peptide segment. SH2 domains consist of approximately 100 amino acids and bind to phosphotyrosine (pTyr)-containing proteins in a sequence dependent manner, while SH3 domains bind to proline-rich sequences in peptides. The association of an SH2 domain with a pTyr-containing sequence of another protein is believed to initiate a complex cascade of intracellular molecular interactions (signals), which effect a wide range of processes including cell growth, proliferation, mitogenisis, and transformation.[1−3] Phosphoproteins which have been shown to bind to the Src SH2 domain include middle T antigen, PDGF receptor, EGF receptor, and focal adhesion kinase.[4−8] Furthermore, Src has been implicated to play a role in both breast cancer[5] and osteopetrosis,[9,10] suggesting that Src might be an attractive therapeutic target.

We have chosen to focus our drug design efforts on the Src SH2 domain since its three-dimensional structure was the first to be determined by X-ray crystallography and since SH2 domains recognize short synthetic pTyr-containing peptides, in which specificity is conveyed by the residues immediately C-terminal to the pTyr residue.[11,12] For Src the optimal binding sequence was found to be -pTyr-Glu-Glu-Ile-. Extensive crystallographic studies have provided a detailed molecular map of both complexed and uncomplexed forms of the Src SH2 protein.[13−15] Since that time, the three-dimensional structures of numerous SH2 domains have also been solved in both liganded and apo-protein forms by X-ray crystallography and NMR techniques.[16] Structurally, all SH2 domains studied thus far are comprised of a central antiparallel β-sheet core flanked on each side by an α-helix. In the reported Src structures, as in other SH2 structures, the phosphopeptide ligands bind perpendicular to the β-sheet core and interact with two well-defined pockets, the pTyr (pY) pocket and the hydrophobic binding pocket (pY+3). Using the three-dimensional X-ray structure of Src SH2 domain complexed to the 11-mer phosphopeptide, Glu-Pro-Gln-pTyr-Glu-Glu-Ile-Pro-Ile-Tyr-Leu, a structure-based design approach has been employed to discover small molecule Src SH2 ligands. The first reported efforts reduced the 11-mer peptide to a potent pentapeptide,[17] and then later to a homologated D-amino acid containing tripeptide.[18] Previously, we have communicated our design of a series of D-amino acid containing tripeptide ligands,[19] a series of dipeptide ligands,[20] and our efforts to modify the pTyr residue.[21,22]

Our motivation for reducing the size, charge, and peptide character of these ligands, while maintaining the potency, is derived from the fact that SH2 domains are intracellular targets requiring the ligands to penetrate cell membranes. Ultimately, inhibition of SH2−phosphoprotein interactions by such small molecules will aid biological proof-of-concept studies which may lead to the development of novel therapeutic agents designed to attenuate Src SH2 specific signal transduction pathways. In this paper, we describe the synthesis, binding affinity, and Src SH2 cocrystal structure of a novel nonpeptide, urea-containing ligand for the Src SH2 domain.

Chemistry

The known pentapeptide,[17] **1**, was synthesized using solid-phase methodology based on an Fmoc/*tert*-butyl protection strategy.[23] The resin for the synthesis of **1** was split prior to the incorporation of the final tyrosine residue, allowing incorporation of tyrosine mimic, **8**, to yield compound **2**. The tyrosine mimic (*R*)-2-(*p*-hydroxybenzyl) succinic acid, **8**, was synthesized by adapting the known Evans methodology-based synthesis of the related phenylalanine mimic.[24] The synthesis of tripeptide **3**, dipeptide **4**, and the protected amine **9**, used in the synthesis of Src SH2 ligands **5** and **6**, has been previously reported.[20] The intermediate **9** was deprotected providing the amine **10** which was employed, without purification, in conjunction with *N*-(*p*-

[⊗] Abstract published in *Advance ACS Abstracts,* October 15, 1997.

S0022-2623(97)00402-0 CCC: $14.00

Scheme 1[a]

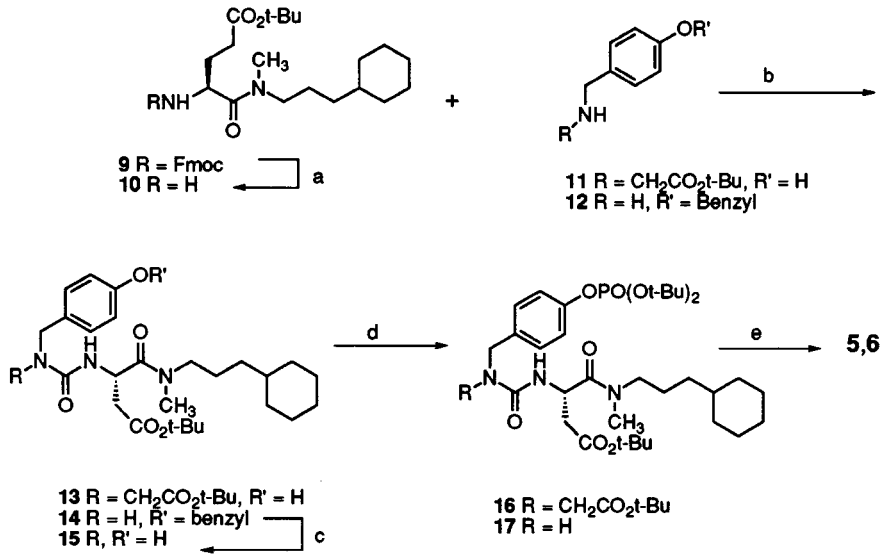

[a] (a) 20% piperdine, CH_2Cl_2, 20 min; toluene, evaporate; (b) ref 25; (c) H_2, 5% Pd on C THF/MeOH; (d) THF, di-*tert*-butyl diethylphosphoramidite, tetrazole, then *t*-BuOOH; (e) CF_3CO_2H:CH_2Cl_2:H_2O (95:4.5:0.5).

Scheme 2[a]

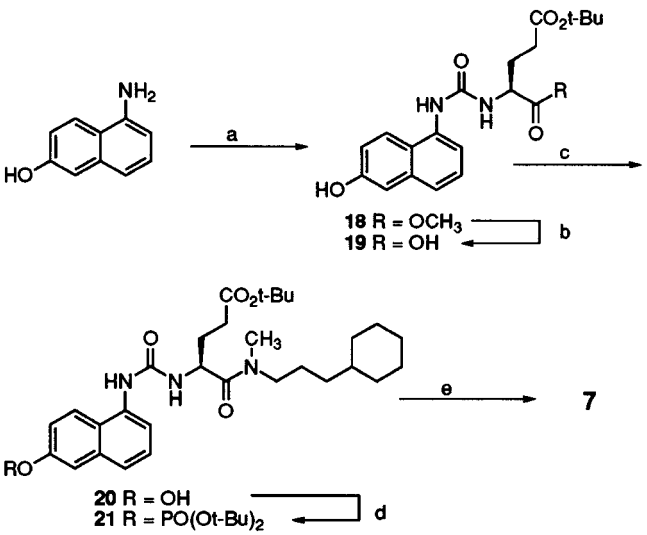

[a] (a) HCl·Glu(Ot-Bu)OMe, ClCOCl in toluene, pyridine, CH_2Cl_2, 0 °C, then 6-amino-1-naphthol; (b) KOH, H_2O/MeOH; (c) methyl(3-cyclohexylpropyl)amine, EDCI, HOBT, *N*-Me-morpholine; (d) CH_2Cl_2, di-*tert*-butyl diethylphosphoramidite, tetrazole; *t*-BuOOH; (e) CF_3CO_2H:CH_2Cl_2:H_2O (95:4.5:0.5).

hydroxybenzyl) glycine *tert*-butyl ester, **11**, to form urea **13** using the methodology of Nowick (Scheme 1).[25] Likewise, amine **10** was employed in conjunction with 4-(benzyloxy)benzylamine **12** to form urea **14**. Hydrogenolysis of the benzyl protecting group in **14** gives the phenol **15** (Scheme 1). The naphthylurea-containing Src SH2 ligand, **7**, (Scheme 2) was synthesized by first reacting Glu(OtBu)-OMe in dichloromethane and excess pyridine with phosgene in toluene to form the isocyanate, which was subsequently coupled with 1-amino-6-naphthol to give urea **18**. The methyl ester of **18** was hydrolyzed, and the resulting acid, **19**, was coupled with methyl (3-cyclohexylpropyl)amine to provide urea **20**. The phenol functionality in **13**, **15**, and **20** was phosphorylated by employing di-*tert*-butyl diethylphosphoramidite and tetrazole (Schemes 1 and 2). The phosphitylated phenol was directly oxidized in situ with *tert*-butyl hydroperoxide, providing the protected phosphates **16**, **17**, and **21**, which could be isolated but were typically directly deprotected with 95:4.5:0.5, trifluoroacetic acid:dichloromethane:water. Purification of the crude phosphorylated Src SH2 ligand was accomplished by reversed phase preparative HPLC providing **5**, **6**, and **7**.

Results and Discussion

Design Strategy. Recently, we have demonstrated the cellular delivery of a series of dipeptide Src SH2 ligands.[26] This was accomplished by replacement of the phosphate group of pTyr, which is expected to be dephosphorylated by nonspecific phosphatases inside cells, by the nonhydrolyzable 4-(phosphonodifluoromethyl)phenylalanine (F_2Pmp) group.[27,28] The F_2Pmp group, which is also dianionic at physiological pH, is then masked as the (acyloxy)methyl ester to provide prodrugs which both penetrate cells and are readily reconverted to the parent Src SH2 ligands inside the cell.

Further development of small effective Src SH2 ligands, which both penetrate cells and provide insight into the therapeutic potential of blocking SH2 domain−phosphoprotein interactions, may hinge on discovering simplified pTyr replacements which ideally would be uncharged and achiral. To this end we synthesized a number of Ac-pTyr analogues[21,22] and incorporated them into the pTyr-Glu-Glu-Ile-Glu sequence for convenient comparison to previously studied phosphate replacements reported by Glaxo researchers.[17] The most potent Ac-Tyr mimic, **8**, was obtained by replacing the acetamide group with an α-carboxymethyl group providing analogue **2** which was equipotent with the parent compound, **1**, Ac-pTyr-Glu-Glu-Ile-Glu (Table 1). Molecular modeling of **2** suggests that potency is retained due to the N-terminal carboxy group forming a bifurcated hydrogen bond to the side chain of Arg 12 just as the acetamide group does in the pentapeptide, **1**, complex.[17] A similar hydrogen bond was seen in the X-ray structure of the D-amino acid containing tripeptide **3** complexed to Src SH2.[32]

Rather than incorporating the (*R*)-(*p*-hydroxybenzyl) succinic acid, **8**, Tyr mimic used in peptide **2** into our dipeptide series of compounds, simplification by removing the chiral center appeared advantageous since the achiral *N*-(*p*-hydroxybenzyl)glycine analogue was readily

Table 1

Compound Number	Structure	IC_{50} (μM)	Tyrosine mimic
1	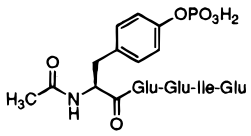	0.5	———
2	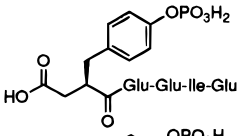	0.4	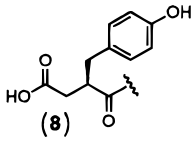 (8)
3	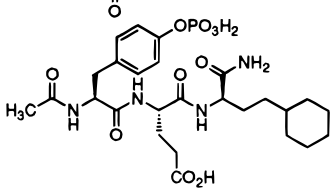	1.8	———
4	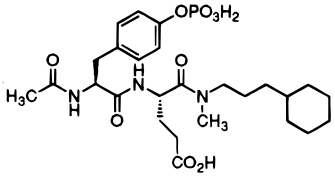	0.8	———
5	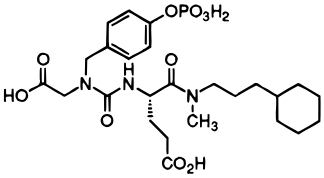	7.0	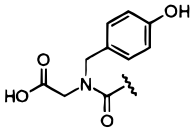
6	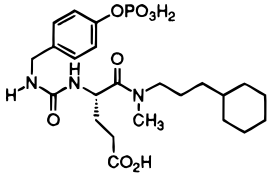	12	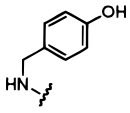
7	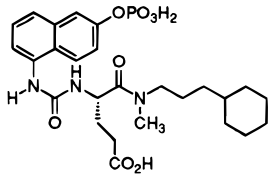	13	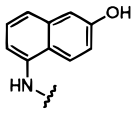

synthesized.[30,31] The protected achiral Tyr mimetic **11** was substituted for the Ac-Tyr group in dipeptide **4** (IC_{50} = 0.8 μM) to provide **5** (IC_{50} = 7.0 μM) resulting in about a 10-fold loss of potency (Table 1). Initially, this drop in potency was hypothetically attributed to the achiral sp^2-hybridized urea linkage causing a ligand conformation unfavorable for optimal binding. Structurally, loss of the sp^3 hybridized chiral center could cause the phosphate group to be poorly positioned in the pY pocket. Alternatively, the urea linkage could cause the N-terminal carboxy group to be outside hydrogen bonding distance with the Arg 12 side chain. Modeling predicted that the carboxy group of **5** was capable of forming a bifurcated hydrogen bond with the Arg 12 side chain while the phosphophenyl group occupied the pY pocket. However, other interactions might be compromised.

To directly evaluate the role of the carboxy group in ligand binding, the Tyr mimic **11** was further simplified to *p*-hydroxybenzylamine providing the nonpeptide Src SH2 ligand **6** (Table 1). Importantly, **6** (IC_{50} = 12 μM), which lacks the carboxymethyl group of **5**, is only about 2-fold less potent than **5**. This suggests that the loss of binding affinity of **5** and **6** relative to dipeptide **4** is likely attributable not only to a conformational effect induced by the achiral urea on the position of the phenyl phosphate group but also to a diminished interaction of the carboxy group of **5** with Arg 12—an interaction not possible with **6** which lacks the carboxy group.

To explore the effect of restricting the conformational freedom of the *p*-hydroxybenzylamine derived portion of **6**, 1-amino-6-naphthol was employed next as a Tyr mimic (Table 1). This modification, in conjunction with the urea linkage, restricts rotational freedom of ligand **7** from the glutamic acid NH through to the phosphate group (as compared to the Ac-pTyr dipeptide analogue **4**). Nonpeptide **7** (IC_{50} = 13 μM) is equipotent with **6**, demonstrating that the increased size and decreased rotational freedom imposed by the naphthol-based Tyr mimic is accommodated by the phosphate binding pocket of Src SH2. These results also suggest that this pocket is somewhat adaptable. The approximate 10-fold difference in binding affinity between **4** and nonpeptides **5**, **6**, and **7**, which contain a diverse set of Ac-Tyr mimics, may be partially attributed to diminished hydrogen-bonding interactions of these Tyr mimics, relative to Ac-Tyr, with the Arg 12 side chain. Even

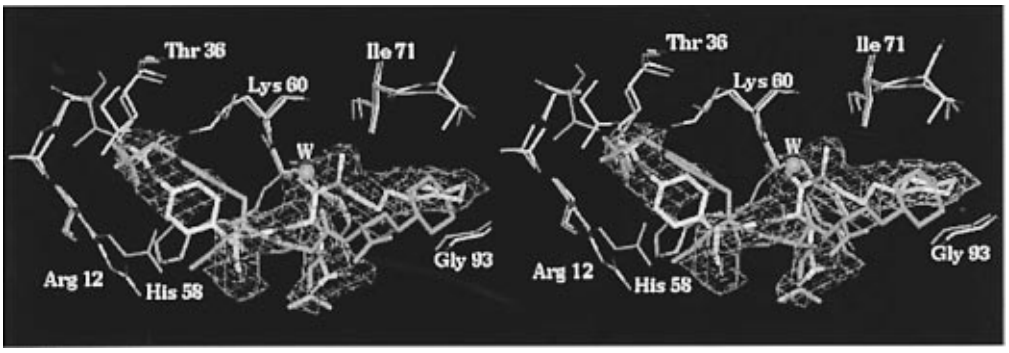

Figure 1. Divergent stereoview of X-ray structures for binding sites of Src SH2 bound to urea **5** (colored by atom type: C, yellow; O, red; N, blue; P, white) and tripeptide **3** (colored cyan). The structural water of the tripeptide complex is shown as a cyan sphere and is labeled as "W". The initial 2.4 Å residual map for urea **5** (colored magenta) is contoured at 3σ and superimposed over the final model of the ligand.

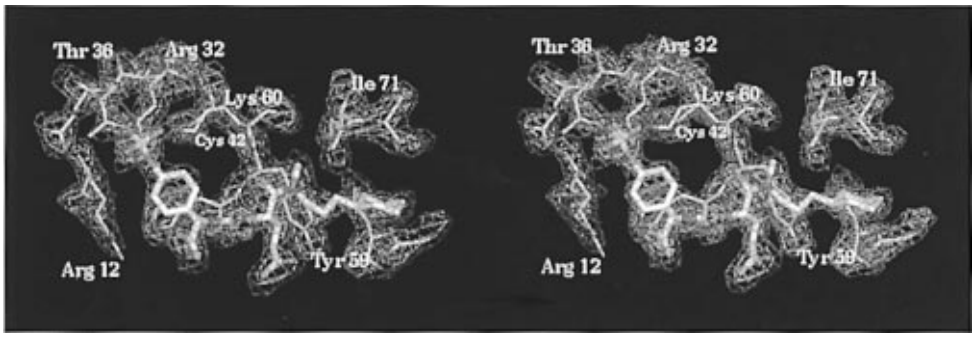

Figure 2. Divergent stereoview of the refined 2.4 Å $2F_o - F_c$ electron density map showing bound ligand (thick bonds) and the surrounding protein residues (thin bonds). The map is contoured at 1σ and 2σ.

with a somewhat adaptable pTyr binding pocket, poor positioning of the phosphate in the binding pocket could also play a role in the diminished binding affinity.

Crystal Structure of Urea 5. To gain an understanding of the nature of the interactions between the SH2 domain and the nonpeptide ligands **5** and **6**, cocrystallization experiments were conducted. A crystal structure of **5** complexed with Src SH2 was determined. An initial $F_o - F_c$ residual map, phased on the molecular replacement solution without ligand, shows the urea compound **5** in good detail (Figure 1). The overall structure of the SH2 domain in the complex is very similar to that previously described,[13,14,17] and the quality for the final 2.4 Å $2F_o - F_c$ map is excellent, as it fully describes both the protein and ligand (Figure 2). Src SH2 residues 107−112 are disordered according to the electron density map and are therefore not included in the final model.

The X-ray results do reveal, however, a unique ligand binding mode which is different than that previously reported for Src SH2 peptide ligands, including the dipeptide **4**[32] and the tripeptide **3**.[32] Although ligand **5** binds with the phosphate group in the pY pocket and the cyclohexyl group in the hydrophobic pY + 3 pocket, as expected, the conformation of the ligand is quite different than initial predictions (Figure 1). In particular, the orientation of the phenyl phosphate ring in the pY pocket is nearly perpendicular to that exhibited by tyrosine-containing peptide ligands, although the phosphate group is centered within 1 Å of that observed for the peptide ligands. Also, as if to avoid a steric clash with the phenyl phosphate ring, the guanadinium of Arg 12 moves away from the pY pocket by several angstroms and, as a result, is not able to form the expected hydrogen bond with the ligand N-terminal carboxymethyl group, leaving it completely exposed to solvent. The side chain of Lys 60 also moves to accommodate the difference in phosphophenyl binding.

Most surprising is the existence of a *cis*-amide linkage between the pY + 1 Glu and the C-terminal methyl (3-cyclohexyl propyl) amine group with respect to dipeptide **4**[32] which has this group trans-oriented. As a result of this unexpected configuration, the structural water molecule (shown as sphere in Figure 1), which usually mediates a hydrogen bond between the Lys 60 backbone and the pY + 1 ligand carbonyl of more peptidic Src SH2 ligands,[13,14,17] is displaced by the *cis*-amide carbonyl oxygen to provide a new direct protein−ligand contact. The hydrogen bond between His 58 carbonyl and the pY + 1 Glu NH observed in all other reported peptide complexes is preserved in the ureido complex, as is the solvent-exposed environment of the pY + 1 Glu side chain. The C-terminal cyclohexyl ring of **5**, however, does not bind as deeply into the pY + 3 pocket as does the preferred Ile residue of the high affinity pY-E-E-I-E sequence, but more deeply than the cyclohexyl group of the tripeptide **3**.

Figure 3 shows the hydrogen bond and van der Waals contacts made by the urea ligand with the Src SH2 domain. In spite of the unique binding mode for the phenyl phosphate group within the pY pocket, the phosphate moiety assumes the same position, but has a different relative orientation, when compared with the phosphate of other Src SH2 ligand complexes (Figure 1). The same pY pocket side chains are involved in the hydrogen-bonding scheme of the phosphate with the exception of Cys 42 and Lys 60, each of which makes contact with a phosphate oxygen in the urea complex, but not in other peptide complexes. However, Arg 12 does not make a hydrogen bond with the phosphate of the urea ligand while Arg 12 does in other crystal complexes reported.

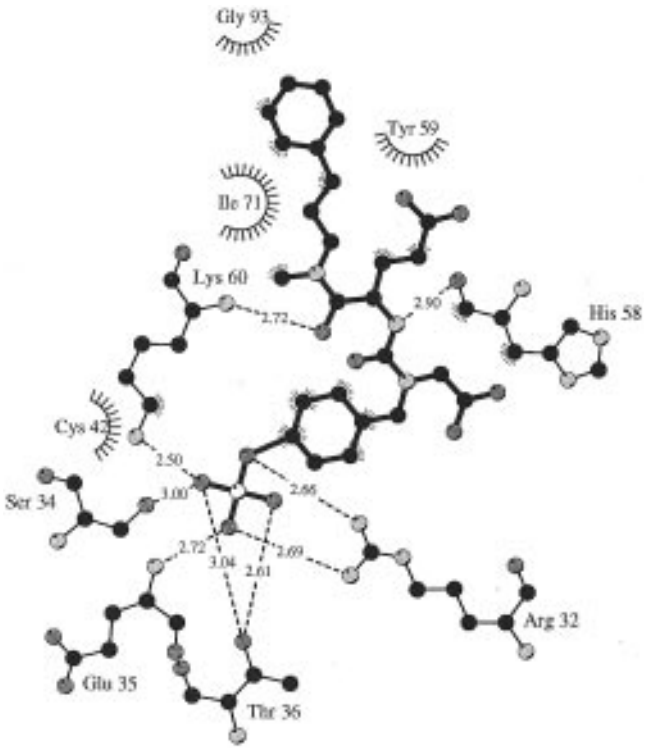

Figure 3. LIGPLOT[38] representation of hydrogen bonds (dashed lines) and van der Waals contacts (spiked partial circles) made by urea **5** (thick bonds) and Src SH2 domain (thin bonds). The gray color scale: phosphorus, white; nitrogen, light; oxygen, medium; carbon, dark.

Conclusions

On the basis of the structural information provided by the X-ray analysis of the complex, the 10-fold difference is potency between ligands **4** and **5** can probably be attributed to several factors: (1) the lack of interaction between the SH2 Arg 12 side chain and both the N-terminal carboxy moiety and the phosphate group of the ligand **5**, (2) the difference in the phosphate binding pattern in the pY pocket, and (3) the displacement of the structural water of the peptide complexes with the *cis*-amide carbonyl. In spite of the decrease in potency, we have successfully designed a series of nonpeptide Src SH2 ligands which contain simplified Tyr mimics. The design was based on modeling of dipeptide **4** in the context of the tripeptide **3** crystal complex. These mimics may aid in the discovery of small effective Src SH2 ligands, which penetrate cells and block Src SH2−phosphoprotein interactions. The crystal structure of **5** complexed with Src SH2 domain reveals some important and unique binding interactions not observed in the complex with tripeptide **3**. Both the orthogonally orientated phenyl phosphate group in the pY pocket and the unique conformation of the solvent-replacing *cis*-amide backbone suggest that a potent nonpeptide Src SH2 ligand need not be strictly modeled after the conventional peptide binding mode. An understanding of these differences may enable us to design more potent and further simplified Src SH2 ligands.

Experimental Section

Inhibition of [^{125}I]Phosphopeptide Binding to Immobilized Src SH2. The binding affinities of compounds tothe *v*-Src SH2 domain was determined using a competitive radiolabeled phosphonopeptide displacement assay. Specifically, binding of ^{125}I-labeled Glu-Pro-Gln-F_2Pmp-Glu-Glu-Ile-Pro-Ile-Tyr-Leu to a glutathione-*S*-transferase(GST)−*v*-Src SH2 fusion protein was performed in 20 mM Tris (pH 7.5), 150 mM NaCl, 5 mM EDTA, and 0.1% NP-40. Assay additions to a Millipore filter plate (0.45 mM PVDF) resulted in *v*-Src SH2 fusion protein−glutathione sepharose bead complex, 2.8 nm [^{125}I]phosphopeptide and 2% DMSO + test compound at different concentrations. Binding was performed at room temperature for 20 min while continuously inverting the plate. Unbound [^{125}I]phosphopeptide was separated from SH2-bound radiolabeled peptide by vacuum filtration and washing two times with 100 μL per well of assay buffer. Results are expressed as IC_{50} values and are averages of at least two duplicate determinations.

X-ray Methods. As described,[29] our *v*-Src SH2 domain was expressed in *E. coli* as a 112-amino acid protein and stored as an ammonium sulfate precipitate slurry (70%). A sample of the slurry was dialyzed against 100 mM NaCl, 10 mM Tris·HCl, pH 7, and concentrated to 30 mg/mL. The complex of Src SH2 with the urea compound **5** was crystallized at room temperature by vapor diffusion in a hanging drop consisting of mother liquor, protein, and 4 mg/mL ligand in a 4:4:2 ratio, with the mother liquor being 20% PEG 6000 and 100 mM sodium cacodylate, pH 6. Hexagonal rods (0.35 mm × 0.1 mm × 0.1 mm) appeared within a week. X-ray diffraction data were collected on a MarResearch image plate, mounted on a Rigaku 200B rotating anode generator (operating at 40 kV and 120 mA) and a graphite monochromator. The data were processed using the XDS package[33] to determine the space group as $P6_1$ with one molecule in the unit cell and cell dimensions $a = b = 74.4$ Å, $c = 38.8$ Å ($V_M = 2.2$ Å^3/Da). Using a detector distance of 100 mm and 1200 s/frame exposures, 95.5% of data 2.4−20.0 Å was collected (4692 unique reflections) with an *R*-merge of 10.5% and a multiplicity of four. The crystal structure of the complex was determined by AmoRe molecular replacement methods[34] using 3.5−10 Å data and the Src SH2 molecule in complex with the 11-mer phosphopeptide[13] as a search model. The search model did not contain the phosphopeptide or the water molecules. The unambiguous molecular replacement solution gave a correlation coefficient of 60.5% and an *R* factor of 36.2%. An initial 2.4 Å $F_o - F_c$ electron density map, phased on the molecular replacement solution, confirmed the correct solution had been found since density in the binding site closely resembled the urea compound **5**. The structure was refined at 2.4 Å resolution using conventional refinement (positional and independent *B* factor) in XPLOR[35] and manual model building was performed in QUANTA[36] on a Silicon Graphics Indigo2 workstation. Waters were added to the model as the quality of the maps allowed. The final *R* factor was 20% with 67 water molecules. Overall deviations from ideal geometry for bonds, angles, planes, and impropers were 0.014 Å, 2.9°, 2.9°, and 28.6°, respectively. The coordinates for the complex have been deposited in Brookhaven DataBank.

Chemistry. General. ^{1}H NMR spectra were recorded on either a Varian XL300 or Unity 400 spectrometers in DMSO-d_6 (DMSO) unless otherwise indicated. ^{31}P NMR spectra were obtained on a Varian Unity 400 spectrometer using a 5 mm Nalorac Quad probe. Spectra were obtained at 293 K, and phosphorus chemical shifts are referenced to external H_3PO_4 in $CDCl_3$ at 0.0 ppm. Chemical ionization mass spectra were recorded on a Fisons (VG Biotech) Trio-2A using 1% ammonia in methane as the reagent gas. Electrospray and APCI mass spectra were obtained on a single quadrapole instrument (VG Fisons Trio 2000). Flash silica gel chromatography was performed using Keiselgel 230−400 mesh. Analytical HPLC chromatograms were obtained using a C18 analytical column (Vydac, 4.6 × 250 mm), eluting with a linear gradient of 0−66% acetonitrile containing 0.1% TFA and water containing 0.1% TFA over 22 min unless otherwise indicated, and the peaks were detected at 214 nm. Thin-layer chromatography employed EM Science silica gel 60 F254 glass backed plates. Tetrahydrofuran (THF) was dried over sodium−benzophenone ketyl and distilled. All other commercially available solvents and reagents were used without further purification. The synthesis of compounds **1**, **3**, and **4** have been previously described.[17,19,20]

Synthesis of Peptides 1, 2, and 3. The nonphosphorylated peptides were prepared by standard solid-phase synthetic

methodology employing a manual shaker. The peptides were assembled using (4-(hydroxymethyl)phenoxy)methyl (HMP) polystyrene resin to give the C-terminal carboxylic acid derivatives or 4-[(2′,4′-dimethoxyphenyl)-Fmoc-aminomethyl]-phenoxy (Rink) resin for the C-terminal carboxamide derivative (giving compound **3**)[19] and were synthesized using Fmoc/*tert*-butyl strategy with 1-hydroxybenzotriazole/diisopropylcarbodiimide mediated coupling in *N*-methylpyrrolidinone. The resin was split after coupling the first four protected amino acids (Glu-Glu-Ile-Glu-resin) to allow incorporation of Ac-Tyr to give known **1**[17] or the Tyr mimic **8**. The tyrosine residue (or mimic) was incorporated with the phenolic residue unprotected, allowing phosphorylation on the resin. Phosphorylation was accomplished using di-*tert*-butyl *N*,*N*-diethylphosphoramidate (50 equiv) and tetrazole (150 equiv) in anhydrous tetrahydrofuran followed by oxidation with *tert*-butyl hydroperoxide according to a described procedure.[37] The peptide was cleaved from the resin using TFA/water/thioanisole (20:1:1, v/v). The phosphopeptide **2** was isolated by preparative reversed phase HPLC. HPLC 100%, t_R = 11.4 min, C18, eluting with a gradient of 0−66% acetonitrile containing 0.1% TFA, and water containing 0.1% TFA over 22 min. Electrospray mass spectrum (50/50 acetonitrile/water + 0.1% ammonium hydroxide) *m*/*z* 804 (M − H). Anal. ($C_{32}H_{54}N_4O_{18}P_1$·(0.50)H_2O·(0.91)TFA·(0.46)CH_3CN) C, H, N.

4-[3-(Carboxymethyl)-3-[4-(phosphonooxy)benzyl]ureido]-4-[(3-cyclohexylpropyl)methylcarbamoyl]butyric Acid (5). (Step 1) To Glu(OtBu)-N(Me)-3-cyclohexylpropyl, **10** (360 mg, 1.0 mmol), synthesized as previously described,[20] ice, dichloromethane (20 mL), and saturated sodium bicarbonate (20 mL), in a separatory funnel was added phosgene in toluene (7.5 equiv). The mixture was shaken for 5 min, and then the organic layer was separated, dried over magnesium sulfate, and concentrated to give the isocyanate as a colorless oil. The isocyanate was treated in dichloromethane (20 mL) with (4-hydroxybenzyl)glycine *tert*-butyl ester, **11** (250 mg, 1.0 mmol), and triethylamine (0.15 mL, 1.0 mmol) for 1 h. Ethyl acetate was added, and the reaction mixture was washed with 10% sulfuric acid, then water, and then brine. After the mixture was dried over magnesium sulfate, the solvent was removed under reduced pressure to give the urea **13** as a colorless oil (500 mg, 83%): ^{1}H NMR (400 MHz) 0.92 (m, 2H), 1.20−2.20 (m, 5H), 1.40 (s, 18H), 1.50−1.70 (m, 10H), 2.22 (m, 2H), 2.90, 3.05 (s, 3H, rotational isomers), 3.10−3.42 (m, 2H), 3.83 (m, 2H), 4.40 (m, 2H), 4.80 (m, 1H), 5.57 (dd, 1H), 6.73 (d, 2H), 7.05 (d, 2H); APCI MS (1:4, methanol/acetonitrile) *m*/*z* calcd 603.7, found 604.5 $[M + H]^+$.

(Step 2) The crude urea **13** was phosphitylated, oxidized, deprotected, and purified in a manner similar to that previously described,[20] giving **5** (49 mg) as a colorless solid: ^{1}H NMR (400 MHz) 0.92 (m, 2H), 1.03−1.25 (m, 6H), 1.42 (m, 1H), 1.62 (m, 7H), 1.78 (m, 1H), 2.24 (t, 2H), 2.79, 3.00 (s, 3H, rotational isomers), 3.02−3.42 (m, 2H), 3.82 (m, 2H), 4.41 (m, 2H), 4.55 (m, 1H), 6.53 (dd, 1H), 7.10 (d, 2H), 7.23 (d, 2H); ^{31}P NMR −5.57; HPLC 100%, t_R 17.4 min, C18, eluting with a gradient of 0−66% acetonitrile containing 0.1% TFA and water containing 0.1% TFA over 22 min. Electrospray mass spectrum (50/50 acetonitrile/water + 0.1% ammonium hydroxide) *m*/*z* calcd 571.5, found 570.3 (M − H). Anal. ($C_{25}H_{38}N_3O_{10}P_1$·(0.13)H_2O·(0.74)TFA) C, H, N.

(*S*)-4-[(3-Cyclohexylpropyl)methylcarbamoyl]-4-[3-[4-(phosphonooxy)benzyl]ureido]butyric Acid (6). (Step 1) Compound **6** was synthesized in a manner similar to that described for **5** only 4-benzyloxybenzylamine, **12**, was reacted with the isocyanate to provide **14**: ^{1}H NMR (300 MHz) 0.80 (m, 2H), 1.10 (m, 6H), 1.37 (s, 9H), 1.20−1.80 (m, 9H), 1.90 (m, 2H), 2.77, 2.98 (s, 3H, rotational isomers), 3.03−3.40 (m, 2H), 4.10 (d, 2H), 4.60 (m, 1H), 5.05 (s, 2H), 6.14 (dd, 1H), 6.40 (dt, 1H), 6.90−7.42 (m, 9H); electrospray mass spectrum (50/50 acetonitrile/water + 0.1% ammonium hydroxide) *m*/*z* calcd 579.7, found 580.5 (M − H).

(Step 2) **14** (520 mg, 0.90 mmol) was dissolved in THF/methanol (4:1, 50 mL), 5% Pd/C (10%) was added, and the mixture was place under 1 atm of hydrogen for 12 h. The reaction was stopped prematurely to avoid possible hydrogenolysis of the benzylurea. The ^{1}H NMR spectra indicated a mixture of the starting material **14** and the phenol **15** were present.

(Step 3) The phenolic hydroxyl group in **15** was phosphitylated, oxidized, deprotected, and purified in a manner as previously described.[20] Preparative reversed phase HPLC of 150 mg of crude **6** gave pure product (42 mg) as a colorless solid after lyophilization: ^{1}H NMR (400 MHz) 1.10 (m, 2H), 1.03−1.26 (m, 5H), 1.40−1.85 (m, 10H), 2.22 (m, 2H), 2.80−3.01 (s, 3H, rotational isomers), 3.10−3.50 (m, 2H), 4.17 (m, 2H), 4.61 (m, 1H), 6.19 (m, 1H), 6.51 (dt, 1H), 7.07 (d, 2H), 7.18 (d, 2H); ^{31}P NMR −5.52; HPLC 98%, t_R = 17.8 min, C18, eluting with a gradient of 0−66% acetonitrile containing 0.1% TFA, and water containing 0.1% TFA over 22 min; electrospray mass spectrum (50/50 acetonitrile/water + 0.1% ammonium hydroxide) *m*/*z* calcd 513.5, found 512.6 (M − H) Anal. ($C_{23}H_{36}N_3O_8P_1$·(0.18)H_2O·(0.25)TFA) C, H, N.

4-[(3-Cyclohexylpropyl)methylcarbamoyl]-4-[3-[6-(phosphonooxy)naphthalen-1-yl]ureido]butyric Acid (7). (Step 1) To H-Glu(OtBu)-OCH_3 (2.0 mmol, 0.50 g) in dichloromethane (25 mL) at 0 °C was added pyridine (8 mmol, 0.66 mL) which was followed by dropwise addition of phosgene in toluene (3.0 mmol, 1.60 mL, 1.92 M). After the mixture was stirred at 0 °C for 2 h, 1-amino-6 naphthol (2.0 mmol, 0.32 g) in dichloromethane was added. After an additional 12 h of stirring at room temperature, the reaction mixture was evaporated to dryness and purified on silica gel (1:19, methanol/dichloromethane) to provide ester **18** as a light brown solid (0.71 g, 88%): ^{1}H NMR (400 MHz) 1.40 (s, 9H), 1.85 (m, 1H), 2.00 (m, 1H), 2.35 (m, 2H), 3.66 (s, 3H), 4.33 (m, 1H), 7.11 (m, 2H), 7.34 (m, 2H), 7.69 (d, 1H), 7.92 (d, 1H); CI MS (1%NH_3 in CH_4) *m*/*z* calcd 402.3, found 403.4 $[M + H]^+$.

(Step 2) To (6-hydroxynaphthalen-1-yl)ureido-L-Glu(OtBu)-OCH_3 **18** (5 mmol, 2.0 g) was added potassium hydroxide (5 mmol, 0.28 g) in water (7 mL). After being heated at 50 °C for 36 h, the reaction mixture was evaporated to dryness. The residue was dissolved in water (15 mL), acidified to pH ∼5 using 0.50 N hydrochloric acid, and extracted with the ethyl acetate (4 × 50 mL) to provide product **19** as a light brown oil (1.20 g, 62%): ^{1}H NMR (300 MHz) 1.52 (s, 9H), 1.98 (m, 1H), 2.16 (m, 1H), 2.43 (m, 2H), 4.38 (m, 1H), 7.05 (d, 1H), 7.21 (m, 2H), 7.24 (m, 2H), 7.90 (d, 2H), 8.10 (d, 1H), 8.75 (s, 1H); electrospray mass spectrum (50/50 acetonitrile/water + 0.1% ammonium hydroxide) *m*/*z* calcd 388.3, found 387.5 (M − H).

(Step 3) (6-Hydroxynaphthalen-1-yl)uredio-L-Glu(OtBu)-OH, **19** (0.50 g, 1.3 mmol), was coupled with methyl (3-cyclohexylpropyl)amine hydrochloride (0.25 g, 1.3 mmol) using the procedure previously reported.[20] The crude product was purified on silica gel (2% methanol/CH_2Cl_2), **20** (0.49 g, 72%): ^{1}H NMR (DMSO/D_2O, 400 MHz) 0.80 (m, 2H), 1.17 (m, 7H), 1.40 (s, 9H), 1.62 (m, 7H), 1.90 (m, 1H), 2.30 (m, 2H), 2.82, 3.07 (s, 3H, rotational isomers), 3.10−3.55 (m, 2H), 4.77 (m, 1H), 7.10 (m, 2H), 7.31 (m, 2H), 7.75 (m, 1H), 7.96 (m, 1H).

(Step 4) The naphthol **20** was phosphitylated, oxidized, deprotected, and purified in a manner similar to that previously described,[20] giving **7** (27 mg): ^{1}H NMR (DMSO/D_2O, 400 MHz) 0.82 (m, 2H), 1.17 (m, 6H), 1.48 (m, 1H), 1.52 (m, 7H), 1.90 (m, 1H), 2.35 (m, 2H), 2.84, 3.08 (s, 3H, rotational isomers), 3.20−3.50 (m, 2H), 4.76 (m, 1H), 7.40 (m, 2H), 7.50 (d, 1H), 7.63 (s, 1H), 7.90 (dd, 1H), 8.10 (dd, 1H); HPLC 100%, t_R 18.9 min, C18, eluting with a gradient of 0−66% acetonitrile containing 0.1% TFA and water containing 0.1% TFA over 22 min; electrospray mass spectrum (50/50 acetonitrile/water + 0.1% ammonium hydroxide) *m*/*z* calcd 549.4, found 548.4 (M − H) Anal. ($C_{26}H_{36}N_3O_8P_1$·(0.3)H_2O)·(0.27)TFA) C, H, N.

(2*R*)-2-[(*tert*-Butyloxycarbonyl)methyl]-3-(4-hydroxyphenyl)propionic Acid (8). Intermediate **8** was synthesized in direct analogy to known procedure:[24] ^{1}H NMR ($CDCl_3$, 400 MHz) 1.42 (s, 9H), 2.37 (m, 1H), 2.55 (m, 1H), 2.72 (m, 1H), 3.00 (m, 2H), 6.76 (d, 2H), 7.04 (d, 2H); APCI MS (1:4, water/acetonitrile) *m*/*z* calcd 280.3, found 279.4 [M − H]. Anal. ($C_{15}H_{20}O_5$) C, H, N.

Acknowledgment. We thank Dr. Gary McClusky and Colleagues for providing the spectroscopic and analytical data. We thank Professor Nowick for generously providing us with his procedure for synthesizing

ureas prior to publication. Finally, we thank Dr. Charles J. Stankovic for helpful discussions and assistance in reviewing the manuscript.

Supporting Information Available: A description of the methods used to produce the *v*-Src protein employed in the crystallization experiments (3 pages). Ordering information is given on any current masthead page.

References

(1) Koch, C. A.; Anderson, D.; Moran, M. F.; Ellis, C.; Pawson, T. SH2 and SH3 domains: elements that control interactions of cytoplasmic signaling proteins. *Science* **1991**, *252*, 668−674.

(2) Cantley, L. C.; Auger, K. R.; Carpenter, C.; Duckworth, B.; Graziani, A.; Kapeller, R.; Soltoff, S. Oncogenes and signal transduction. *Cell* **1991**, *64*, 281−302.

(3) Pawson, T.; Gish, G. D. SH2 and SH3 domains: from structure to function. *Cell* **1992**, *71*, 359−362.

(4) Alonso, G.; Koegl, M.; Mazurenko, N.; Courtneidge, S. A. Sequence requirements for binding of Src family tyrosine kinases to activated growth factor receptors. *J. Biol. Chem.* **1995**, *270*, 9840−9848.

(5) Luttrell, D. K.; Lee, A.; Lansing, T. J.; Crosby, R. M.; Jung, K. D.; Willard, D.; Luther, M.; Rodriguez, M.; Berman, J.; Gilmer, T. M. Involvement of pp60src with two major signaling pathways in human breast cancer. *Proc. Natl. Acad. Sci. U.S.A.* **1994**, *91*, 83−87.

(6) Roussel, R. R.; Brodeur, S. R.; Shalloway, D.; Laudano, A. P. Selective binding of activated pp60c-src by an immobilized synthetic phosphopeptide modeled on the carboxyl terminus of pp60c-src. *Proc. Natl. Acad. Sci. U.S.A.* **1991**, *88*, 10696−10700.

(7) Payne, G.; Shoelson, S. E.; Gish, G. D.; Pawson, T.; Walsh, C. T. Kinetics of p56lck and p60src Src homology 2 domain binding to tyrosine-phosphorylated peptides determined by a competition assay or surface plasmon resonance. *Proc. Natl. Acad. Sci. U.S.A.* **1993**, *90*, 4902−4906.

(8) Payne, G.; Stolz, L. A.; Pei, D.; Band, H.; Shoelson, S. E.; Walsh, C. T. The phosphopeptide-binding specificity of Src family SH2 domains. *Chem. Biol.* **1994**, *1*, 99−105.

(9) Boyce, B. F.; Yoneda, T.; Lowe, C.; Soriano, P.; Mundy, G. R. Requirement of pp60c-src expression for osteoclasts to form ruffled borders and resorb bone in mice. *J. Clin. Invest.* **1992**, *90* (4), 1622−1627.

(10) Soriano, P.; Montgomery, C.; Geske, R.; Bradley, A. Targeted disruption of the c-src proto-oncogene leads to osteopetrosis in mice. *Cell* **1991**, *64*, 693−702.

(11) Songyang, Z.; Shoelson, S. E.; Chaudhuri, M.; Gish, G.; Pawson, T.; Haser, W. G.; King, F.; Roberts, T.; Ratnofsky, S.; Lechleider, R. J.; Neel, B. G.; Birge, R. B.; Fajardo, J. E.; Chou, M. M.; Hanafusa, H.; Schaffhausen, B.; Cantley, L. C. SH2 domains recognize specific phosphopeptide sequences. *Cell* **1993**, *72*, 767−778.

(12) Songyang, Z.; Shoelson, S. E.; McGlade, J.; Olivier, P.; Pawson, T.; Bustelo, X. R.; Barbacid, M.; Sabe, H.; Hanafusa, H.; Yi, T.; Ren, R.; Baltimore, D.; Ratnofsky, S.; Feldman, R. A.; Cantley, L. C. Specific motifs recognized by the SH2 domains of Csk, 3BP2, fps/fes, GRB-2, HCP, SHC, Syk, and Vav. *Mol. Cell. Biol.* **1994**, *14*, 2777−2785.

(13) Waksman, G.; Kominos, D.; Robertson, S. C.; Pant, N.; Baltimore, D.; Birge, R. B.; Cowburn, D.; Hanafusa, H.; Mayer, B. J.; Overduin, M.; Resh, M. D.; Rios, C. B.; Silverman, L.; Kuriyan, J. Crystal structure of the phosphotyrosine recognition domain SH2 of v-src complexed with tyrosine-phosphorylated peptides. *Nature* **1992**, *358*, 646−653.

(14) Waksman, G.; Shoelson, S. E.; Pant, N.; Cowburn, D.; Kuriyan, J. Binding of a high affinity phosphotyrosyl peptide in the Src SH2 domain: Crystal structures of the complexed and peptide-free forms. *Cell* **1993**, *72*, 779−790.

(15) Xu, W.; Harrison, S. C.; Eck, M. J. Three-dimensional structure of the tyrosine kinase c-Src. *Nature* **1997**, *385*, 595−602.

(16) Stankovic, C. J.; Plummer, M. S.; Sawyer, T. K. Peptidomimetic ligands for Src homology-2 domains. In *Advances in amino acid mimetics and peptidomimetics*; Abell, A., Ed.; JAI Press: Greenwich, CT; Vol. 1, pp 127−163 (in press).

(17) Gilmer, T.; Rodriguez, M.; Jordan, S.; Crosby, R.; Alligood, K.; Green, M.; Kimery, M.; Wagner, C.; Kinder, D.; Charifson, P.; Hassel, A. M.; Willard, D.; Luther, M.; Rusnak, D.; Sternbach, D. D.; Mehrotra, M.; Peel, M.; Shampine, L.; Davis, R.; Robins, J.; Patel, I. R.; Kassel, D.; Burkhart, W.; Moyer, M.; Bradshaw, T.; Berman, J. Peptide inhibitors of src SH3−SH2−phosphoprotein interactions. *J. Biol. Chem.* **1994**, *269*, 31711−31719.

(18) Rodriguez, M.; Crosby, R.; Alligood, K.; Gilmer, T.; Berman, J. Tripeptides as selective inhibitors of src-SH2 phosphoprotein interactions. *Lett. Pept. Sci.* **1995**, *2*, 1−6.

(19) Plummer, M. S.; Lunney, E. A.; Para, K. S.; Prasad, J. V. N. V.; Shahripour, A.; Singh, J.; Stankovic, C. J.; Humblet, C.; Fergus, J. H.; Marks, J. S.; Sawyer, T. K. Hydrophobic D-amino acids in the design of peptide ligands for the $pp60^{src}$ SH2 domain. *Drug Des. Disc.* **1996**, *13*, 75−81.

(20) Plummer, M. S.; Lunney, E.; Para, K. S.; Shahripour, A.; Stankovic, C. J.; Humblet, C.; Fergus, J. H.; Marks, J. S.; Herrera, R.; Hubbell, S.; Saltiel, A.; Sawyer, T. K. Design of peptidomimetic ligands for the pp60src SH2 domain. *Bioorg. Med. Chem.* **1997**, *5*, 41−47.

(21) Shahripour, A.; Plummer, M. S.; Lunney, E. A.; Vara Prasad, J.; Singh, J.; Para, K. S.; Stankovic, C. J.; Eaton, S. R.; Marks, J. S.; Decker, S. J.; Herrera, R.; Hubbell, S.; Saltiel, A. R.; Sawyer, T. K. Novel phosphotyrosine and hydrophobic D-amino acid replacements in the design of peptide ligands for pp60src SH2 domain. In *Peptides: Chemistry, Structure and Biology*; Kaumaya, P. T. P., Hodges, R. S., Eds.; Mayflower Scientific Ltd.: Kingswinford, England, 1995; pp 394−396.

(22) Shahripour, A.; Plummer, M. S.; Lunney, E.; Para, K. S.; Stankovic, C. J.; Rubin, J. R.; Humblet, C.; Fergus, J. H.; Marks, J. S.; Herrera, R.; Hubbell, S. E.; Saltiel, A. R.; Sawyer, T. K. Novel phosphotyrosine mimetics in the design of peptide ligands for pp60src SH2 domain. *Bioorg. Med. Chem. Lett.* **1996**, *6*, 1209−1214.

(23) Fields, G. B.; Noble, R. L. Solid-phase peptide synthesis utilizing 9-fluorenylmethoxycarbonyl amino acids. *Int. J. Pept. Protein Res.* **1990**, *35*, 161−214.

(24) Plattner, J. J.; Marcotte, P. A.; Kleinert, H. D.; Stein, H. H.; Greer, J.; Bolis, G.; Fung, A. K. L.; Bopp, B. A.; Luly, J. R.; Sham, H. L.; Kempf, D. J.; Rosenberg, S. H.; Dellaria, J. F.; De, B.; Merits, I.; Perun, T. J. Renin inhibitors. Dipeptide analogs of angiotensinogen utilizing a structurally modified phenylalanine residue to impart proteolytic stability. *J. Med. Chem.* **1988**, *31*, 2277−2288.

(25) Nowick, J. S.; Holmes, D. L.; Noronha, G.; Smith, E. M.; Nguyen, T. M.; Huang, S.-L. Synthesis of peptide isocyanates and isothiocyanates. *J. Org. Chem.* **1996**, *61*, 3929−3934.

(26) Stankovic, C. J.; Surendran, N.; Lunney, E.; Plummer, M. S.; Para, K. S.; Shahripour, A.; Humblet, C.; Fergus, J. H.; Marks, J. S.; Herrera, R.; Hubbell, S. E.; Saltiel, A. R.; Stewart, B. H.; Sawyer, T. K. The Role of 4-Phosphonodifluoromethyl- and 4-phosphono-phenylalanine in the selectivity and cellular uptake of SH2 domain ligands. *Bioorg. Med. Chem. Lett.* **1997**, *7* (14), 1909−1914.

(27) Smyth, M. S.; Ford, H., Jr.; Burke, T. R., Jr. A general method for the preparation of benzylic α,α-difluorophosphonic acids; nonhydolyzable mimetics of phosphotyrosine. *Tetrahedron Lett.* **1992**, *33*, 4137−4140.

(28) Burke, T. R., Jr.; Smyth, M. S.; Otaka, A.; Nomizu, M.; Roller, P. P.; Wolf, G. F.; Case, R.; Shoelson, S. E. Nonhydrolyzable phosphotyrosyl mimetics for the preparation of phosphatase-resistant SH2 domain inhibitors. *Biochemistry* **1994**, *33*, 6490−6494.

(29) Details of the protein preparation used in the crystallography experiments is available as Supporting Information (3 pages). Ordering information is given on any current masthead page.

(30) Zuckermann, R. N.; Martin, E. J.; Spellmeyer, D. C.; Stauber, G. B.; Shoemaker, K. R.; Kerr, J. M.; Figliozzi, G. M.; Goff, D. A.; Siani, M. A.; Simon, R. J.; Banville, S. C.; Brown, E. G.; Wang, L.; Richter, L. S.; Moos, W. H. Discovery of nanomolar ligands for 7-transmembrane G-protein-coupled receptors from a diverse N-(substituted)glycine peptoid library. *J. Med. Chem.* **1994**, *37*, 2678−2685.

(31) Zuckermann, R. N.; Kerr, J. M.; Kent, S. B. H.; Moos, W. H. Efficient method for the preparation of peptoids [oligo(N-substituted glycines)] by submonomer solid-phase synthesis. *J. Am. Chem. Soc.* **1992**, *114*, 10646−10647.

(32) Holland, D. R., personal communication.

(33) Kabsch, W. *Recent extensions of the data processing program XDS*; Proceedings of the CCP4 study weekend; Sawyer, L., Isaacs, N., Bailey, S., Eds.; SERC Daresbury Laboratory: Warrington, U.K., 1993; pp 63−70.

(34) Navaza, J. AmoRe: an automated package for molecular replacement. *Acta Crystallogr.* **1994**, *A50*, 157−163.

(35) Brunger, A. T. *X-PLOR Version 3.1*; Yale University Press: New Haven, 1992.

(36) QUANTA *Users Guide*; v. 4.0 ed.; Molecular Simulations: San Diego, 1996.

(37) McNamara, D. J.; Dobrusin, E. M.; Zhu, G.; Decker, S. J.; Saltiel, A. R. Inhibition of binding of phospholipase Cg1 SH2 domains to phosphorylated epidermal growth factor receptor by phosphorylated peptides. *Int. J. Pept. Protein Res.* **1993**, *42*, 240−248.

(38) Wallace, A. C.; Laskowski, R. A.; Thorton, J. M. *Protein Eng.* **1995**, *8* (2), 127−134.

JM970402Q